pISSN 1738-2696 · eISSN 2212-5469
http://dx.doi.org/10.1007/s13770-015-0001-y
ORIGINAL ARTICLE

TERM

Fabrication of an Osteochondral Graft with Using a Solid Freeform Fabrication System

Soon Sim Yang[1,2], Woo Hee Choi[1,2], Bo Ram Song[1,2], He Jin[1,3], Su Jeong Lee[1,2], Su Hee Lee[4], Junhee Lee[4], Young Jick Kim[1], So Ra Park[5], Sang-Hyug Park[6]*, Byoung-Hyun Min[1,2,3]*

[1]Cell Therapy Center, Ajou University Medical Center, Suwon, Korea
[2]Department of Molecular Science and Technology, Ajou University, Suwon, Korea
[3]Department of Orthopedic Surgery, School of Medicine, Ajou University, Suwon, Korea
[4]Department of Nature-Inspired Nano Convergence System, Korea Institute of Machinery & Materials, Daejeon, Korea
[5]Department of Physiology, College of Medicine, Inha University, Incheon, Korea
[6]Department of Biomedical Engineering, Jungwon University, Goesan, Korea

Current approaches for the engineering of osteochondral grafts are associated with poor tissue formation and compromised integration at the interface between the cartilage and bone layers. Many researchers have attempted to provide osteochondral grafts of combined cartilage and bone for osteochondral repair to help overcome the limitations of standard procedures. Solid freeform fabrication is recognized as a promising tool for creating tissue engineering scaffolds due to advantages such as superior interconnectivity and a highly porous structure. This study aimed to develop a three-dimensional plotting system to enable the manufacturing of a biphasic graft consisting cartilage and subchondral bone for application to osteochondral defects. The material advantages of both synthetic (poly L lactide-co-polyglycolide) and natural (alginate) polymers were combined for a supporting frame and cell printing. Specifically, in order to promote the maturity of the osteochondral graft in our study, cartilage-derived ECM (cECM) or hydroxyapatate (HA) substances blended with alginate was plotted together with human fetal cartilage-derived progenitor cells in the cartilage or subchondral bone layer under a multi-nozzle deposition system. Notably, a plotted biphasic graft shows good integration between cartilage and subchondral bone layers without structural separation. Furthermore, the non-toxicity of the cECM and HA substances were proved from a live/dead assay of plotted cell-laden alginate. A fabricated osteochondral graft with cECM and HA substances showed dominant cartilage and bone tissue formation in a differentiation assay. Future studies should be done to modify the alginate physical properties for long-lasting structural stability.
Tissue Eng Regen Med 2015;12(4):239-248

Key Words: Osteochondral graft; Solid freeform fabrication; Poly (L-lactic acid-co-glycolic acid)/alginate hybrid printing; Cartilage-derived ECM; Human fetal derived progenitor cells

INTRODUCTION

Cartilage tissue plays critical roles in articular movements by decreasing the frictional force or decentering the weight. However, because this tissue is very thin (3–4 mm thin in the case of a human knee joint), it is necessary to transplant subchondral bone for its fixation when transplanting it. It is known that transplanted cartilage is very difficult to integrate with the surrounding cartilage of recipient. According to research by Obradovic et al. [1], bone integration is much faster, and it occurs only two weeks after transplantation, while the integration of cartilage takes more than 24 weeks. Therefore, stable fixation of a cartilage graft is possible by a fixation technique with subchondral bone. Given that the life span and mechanical behavior of cartilage are closely related to the mechanical behavior of subchondral bone, a tissue engineering manufacturing process is also necessary for successful cartilage tissue engineering. Over the last couple of decades, tissue engineers have dedicated themselves to seeding cells onto a porous biodegradable scaffold to induce the functional assembly into three-dimensional (3D) tissues [2,3]. This strategy has achieved notable progress in simple tissue/organ regeneration applications. However, simple

Received: January 6, 2015
Revised: February 26, 2015
Accepted: March 9, 2015
***Corresponding author:** Byoung-Hyun Min, Department of Orthopedic Surgery, School of Medicine, Ajou University, 164 World cup-ro, Yeongtong-gu, Suwon 443-380, Korea.
Tel: 82-31-219-4441, Fax: 82-31-219-4442, E-mail: bhmin@ajou.ac.kr
***Corresponding author:** Sang-Hyug Park, Department of Biomedical Engineering, Jungwon University, 85 Munmu-ro, Goesan-eup, Goesan 367-805, Korea.
Tel: 82-43-830-8609, Fax: 82-43-830-8679, E-mail: shpark@jwu.ac.kr

© The Korean Tissue Engineering and Regenerative Medicine Society

strategies with cell seeding onto a porous 3D scaffold during tissue engineering cannot be used to form complex organs [4]. Many studies have attempted the complex manufacturing of osseous tissue and cartilage tissue. These efforts can be subdivided into the single scaffold type, the hybrid scaffold & hybrid cell type, and the hybrid scaffold & single cell type [5]. Each type has its own advantages, yet on the other hand, they all have limitations. These processes include the inducing of cells from the host tissue, the independent differentiation of cells into bone or cartilage within the tissue, and the integration of two tissues. To realize independent differentiation, it is necessary to use a bioreactor to supply different culture media or to manufacture the bone and cartilage separately and then bond the two tissues, which is technically difficult. However if one could have a scaffold to induce a cell into an osteoblast or a chondrocyte using stem cells, the technical difficulties would be greatly reduced.

Practically, the properties of tissue scaffolds play an important role in controlling the cell response, differentiation, and ultimately, functional tissue regeneration [3,6]. In particular, scaffolds which simulate native tissue could provide a favorable microenvironment in which to facilitate cell attachment, growth, and differentiation. Hence, efforts are increasingly being focused on design and manufacturing technologies which can generate and modify the structures and surfaces of biomaterials [7,8]. Conventional fabrication processes of engineered scaffolds are unable to control precisely the pore size, pore geometry, or pore interconnectivity within the scaffold. In contrast, solid freeform fabrication (SFF) technology can produce scaffolds with fully designed and interconnected pore structures [9,10]. Thus, SFF has recently been introduced as a powerful tool with which to fabricate supporting structures.

The advantage of the SFF approach is that it does not require the construction of layer-specific mold patterns or stamps, which simplifies experimental procedures. The utilization of SFF enables the production of 3D scaffolds with complex geometries and very fine structures [11]. Numerous research groups have developed the SFF process and assembled a plotted 3D architecture using synthetic and natural materials to provide a scaffold for tissue engineering [12,13]. However, only a few materials have successfully been 3D plotted using this technique, such as thermoplastic materials such as polycaprolactone (PCL), poly-L-lactide and poly L lactide-co-polyglycolide (PLGA) [14-16]. Thermoresponsive materials can produce well-designed, plotted scaffolds by 3D plotting owing to their good mechanical properties [17]. On the other hand, synthetic biomaterials have several disadvantages, including the fact that their structures and compositions are not similar to those of native tissues. Moreover, their biocompatibility levels are poor. Thus, natural biomaterials have been developed as an alternative and are preferred due to their inherent advantages for clinical applications [8,18,19]. One typical natural polymer is alginate, which is preferred for SFF fabrication because alginate and calcium chloride solidify rapidly with multivalent cations after mixing [20]. The biocompatibility and cell delivery efficacy of alginate materials have been proven in numerous studies [21-23].

Cell seeding onto an artificial supporter is an important process in tissue engineering manufacturing. Homogeneous cell seeding onto an artificial supporter is extremely difficult, and it becomes more critical when the size of the supporter is larger. Thus, it is difficult to create tissue after homogenous cell culturing. Moreover, cell necrosis occurs in the core area of the supporter, which makes tissue formation even more challenging. Cell printing is becoming a key technique with which to resolve this problem. That is, we can seed simultaneously cells that can be divided into various tissues and then spread them homogenously.

In this study, we developed a 3D plotting system which enables the manufacturing of a biphasic graft consisting of cartilage and subchondral bone for application to osteochondral defects. The hybrid material advantages of both synthetic (PLGA) and natural (alginate) polymers were combined for a supporting structure and for cell printing. Specifically, to induce a mature osteochondral graft, porcine-cartilage-derived ECM (cECM) and hydroxyapatite (HA) substances were blended with alginate containing human fetal-derived stem cells (HFCPCs) for the cartilage and subchondral bone layers, respectively. The current study identified the plotting potential and tissue formation potential of 3D printed cartilage/subchondral bone grafts for regeneration in cases of osteochondral defects.

MATERIALS AND METHODS

Cell culture

HFCPCs were isolated from 12 weeks to 16 weeks fetus limbs. The samples were delivered and processed under sterile conditions. Patients were informed and gave consent, and the experiments followed the guidelines from the Ajou University Medical Center Institutional Review Board (CRO-07-139, Suwon, Korea). The fetal cartilage was minced and then treated with 0.1% of a collagenase solution overnight at 37°C in a 5% CO_2 incubator. Subsequently, cells were centrifuged at 1700 RPM for 10 min after cell-strainer filtering. Cells were re-suspended in DMEM; supplemented with 10% fetal bovine serum (FBS), 100 μL/mL penicillin G and 100 μg/mL streptomycin; and plated onto 100-mm culture dishes at 1.5×10^6 cells/cm^2.

Differentiation of HFCPCs

The HFCPCs at passage 2 were analyzed for their adipogenic, osteogenic, and chondrogenic differentiation ability *in vitro* for 21 days. HFCPCs were planted into six-well plates and a specific induction medium was added 24 hours later. For adipogenesis, cells were plated into a six-well plate at a density of 2×10^5 cells/well. The adipogenic induction medium consisted of complete medium supplemented with 1 μM dexamethasone, 10 μg/mL insulin, 0.5 mM isobutylmethylxanthine, and 0.1 mM indomethacin. After 21 days, the adipogenic cultures were fixed in 4% paraformaldehyde for at least 1 h and stained with fresh Oil Red-O solution for 2 h. For osteogenesis, cells were plated in a six-well plate at a density of 2×10^4 cells/well. The osteogenic induction medium consisted of a-MEM supplemented with 10% FBS, 10 mM b-glycerophosphate, and 50 μM ascorbic acid. These dishes were stained with a fresh 0.5% alizarin red solution.

The chondrogenic differentiation of the mesencymal stem cell (MSC) was demonstrated using a pellet culture system. The second-passaged 5×10^5 MSCs were centrifuged at 500×g for 5 min and the pellet was cultured in 1 mL of DMEM containing 10 ng of TGF-β3 in 15 mL polystyrene conical tubes. After one day, when the cells had aggregated into a round form, the culture medium was changed to a chondrogenic medium consisting of DMEM with 100 U/mL penicillin, 100 μg/mL streptomycin, 100 μg/mL pyruvate, 40 μg/mL proline, 50 μg/mL l-ascorbicacid-2-phosphate, 1% ITS, and 100 nM dexamethasone. The chondrogenic differentiation was evaluated by Safranin-O staining.

Multi-head 3D plotting system

In this study, the 3D SFF plotting system used had multi-head nozzles for dual printing. It was supplied by the department in control of the Nature-Inspired Nano Convergence System at the Korea Institute of Machinery & Materials (Daejeon, Korea) (Fig. 1). In detail, computerized tomography and magnetic resonance images in data are converted into typical stereolithography results from 3D shape data through a conversion program. These data are converted again into NC code, which includes driving information such as the space, direction, height, and speed for plotting the nozzle of the dispenser. The dual-3D SFF plotting system had motion, temperature and pneumatic/mechanical suspending controllers. The temperature and pressure of each head were controlled individually. This equipment consists of a two-head system; one head is a thermo-responsive polymer (PLGA) nozzle for the frame structure and the other head is a natural hydrogel nozzle for cell printing. The plotting system consists of a x, y, and z stage, an air pressure supply, a screw mixing system, a compression controller, and a 3D-data processing program system.

Plotting of biphasic scaffolds for osteochondral grafts

Experimental groups were divided by the dual-printing of PLGA and cell-laden alginate (PLGA/alginate), PLGA and 10% cECM blended cell-laden alginate (PLGA/cECM-alginate), and PLGA and 10% HA-blended cell-laden alginate (PLGA/HA-alginate). A PLGA-only scaffold served as a control. Manufacturing was performed at room temperature, and this process consisted of alternating steps of PLGA and alginate printing. The PLGA (PLA 75:PGA 25, Boehringer Ingelheim, Germany) was heated to 120°C and subsequently dispensed through a 300-μm metal needle at a pressure of 120 kpa and a deposition speed of 120 mm/min. Medium-viscosity sodium alginate [3%, Sigma-Aldrich, in phosphate-buffered saline (PBS, Invitrogen, Carlsbad, CA, USA) and subsequently autoclaved] was dispensed between the PLGA strands, at room temperature, using a deposition speed of 65 mm min-1, a spindle speed of 1.5 and a nozzle diameter of 300 μm. Subsequent layers were deposited at an angle (normally 90°, 0−90) with the underlying layer. After all layers had been printed, the alginate was solidificated with a 5 mM calcium chloride ($CaCl_2$, Sigma-Aldrich) solution for 3 min. Static cell seeding was done after the printing process for the PLGA-only scaffolds. The cell-laden alginate

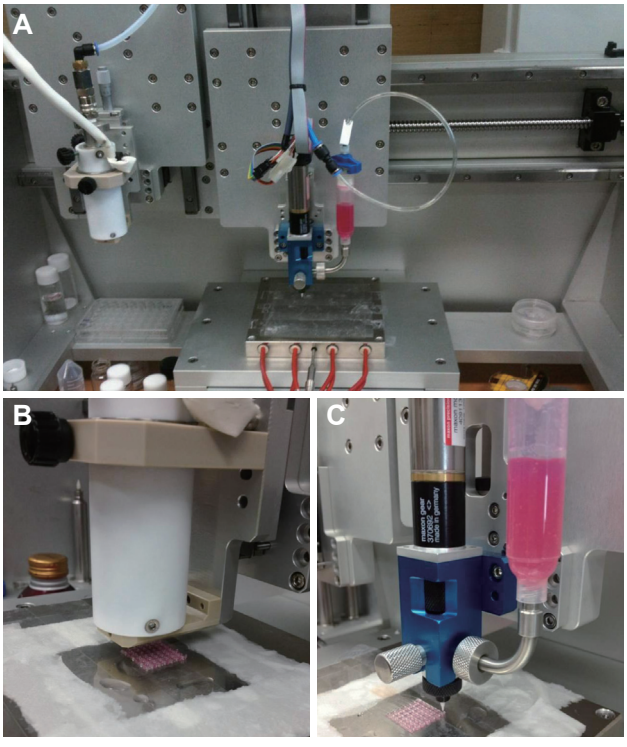

Figure 1. Dual-head printing deposition system (A) a front view of dual head system (B) including a pneumatic pressure supply, a temperature nozzle for thermo-responsive polymer [Poly (L-lactic acid-co-glycolic acid)], and (C) a pneumatic pressure supply and a screw spinning nozzle for cell-laden natural hydrogel (3% alginate).

solution contained 1×10^7 cells/mL for the other groups. Fine cECM and HA ground powders were physically blended into a 3% alginate solution before cell mixing.

SEM analysis and viability analysis

The specimens were freeze-dried and gold-coated with a sputter coater for 60 s. The morphology of the specimens was then analyzed using a scanning electron microscope (SEM, Stereoscan 440, Cambridge, UK) operated at 10 kV. The viabilities of adherent cells on the scaffold and of encapsulated cells in the hydrogel were assessed using a live/dead cell assay kit (Lonza Walkersville, Walkersville, MD, USA). Live and dead cells were represented as green and red fluorescent colors, respectively. The stained cells were imaged and counted manually using fluorescence microscopy to quantify the percentages of live and dead cells (Axiovert 200, Zeiss, Jena, Germany).

Evaluation of differentiation with reverse transcriptase-polymerase chain reaction analysis

Total RNA was extracted using the RNA Easy-Spin Kit (Intron, Seongnam, Korea) following the manufacturer's instructions. RNA of an amount of 1 μg was used for cDNA synthesis using the First-Strand cDNA Synthesis Kit for RT-PCR (AMV) (Rhoche, Mannheim, Germany), and 1 μg of the synthesized cDNA was used for the polymerase chain reaction. The synthesized cDNA (1 μg) was used for PCR using primer sequences of type 2 collagen alpha 1 (Col2A1), aggrecan, alkaline phosphatase (ALP), osteopontin (OPN). Glyceraldehyde-6-phosphate dehydrogenase (GAPDH) was used as an internal control. PCR products were separated on a 1.5% agarose gel and stained with ethidium bromide. They were then visualized and digitalized with the Image Analysis System Gel (Geliance 200, PerkinElmer). The sequences of the primers are listed in Table 1.

Biochemical analysis

Total GAG contents were analyzed using the 1,9-dimethylmethylene blue (DMB) assay technique. Individual samples were mixed with the DMB solution and the absorbance was measured at a wavelength of 525 nm. The total GAG of each sample was extrapolated using a standard plot of shark chondroitin sulfate (Sigma, St. Louis, MO, USA) in the range of 0−50 μg/mL. For a DNA analysis, the scaffolds were chopped by micro-scissors. The DNA contents were measured using the Pico-Green assay. Samples were extracted twice with 0.5 mL of 5% trichloro acetic acid for the total calcium content. The calcium content was determined by a colorimetric assay using the ortho-cresolftaleina complex one Calcium LiquiColor test (Stanbio Laboratory, TX, USA). The calcium complex was measured spectro-photometrically at 575 nm.

The ALP activity assays were done with the p-nitrophenol (pNPP) ALP assay kit (ANASPEC, CA, USA) following the manufacturer's directions. The analysis was performed on Day 14 after *in vitro* culturing. The collected scaffolds were washed three times with PBS, cut down with scissors, and homogenized in lysis buffer. The sample lysate was centrifuged at 10000×g for 15 min at 4°C. The supernatant was assayed for ALP activity using pNPP as a substrate. Into each well of 96-well plates, an aliquot of supernatant and the pNPP mixture were added then incubated at 37°C for 30 min. In addition, stop solution was added the wells to stop the reaction before the absorption was measured. The absorbance of p-NPP was determined at 405 nm using a micro-plate reader (TECAN Infinite 200, Switzerland).

Statistical analysis

The statistical analyses were done using the 'analysis of variance-Tukey' test (SPSS, Chicago, IL, USA) between groups. Statistical significance was assigned as either $p<0.05$ or $p<0.001$.

Table 1. The primers used for RT-PCR

Primer		Sequence	Product size
GAPDH	Forward	5'-GGTCATGAGTCCTTCCACGAT-3'	520 bp
	Reverse	5'-GGTGAAGGTCGGAGTCAACGG-3'	
ALP	Forward	5'-CCACGTCTTCACATTTGGTG-3'	196 bp
	Reverse	5'-AGACTGCGCCTGGTAGTTGT-3'	
Osteopontin	Forward	5'-TTGCAGTGATTTGCTTTT GC-3'	161 bp
	Reverse	5'-GTCATGGCTTTCGTTGGACT-3'	
Type II collagen alpha 1	Forward	5'-GATATTGCACCTTTGGACAT-3'	344 bp
	Reverse	5'-CCCACAATTTAAGCAAGAAG-3'	
Aggrecan	Forward	5'-GAAAGGTGTTGTGTTCCACT-3'	319 bp
	Reverse	5'-GTCATAGGTCTCGTTGGTGT-3'	

RT-PCR: reverse transcriptase-polymerase chain reaction, GAPDH: glyceraldehyde-6-phosphate dehydrogenase, ALP: alkaline phosphatase

RESULTS

Characterization of scaffolds and cell viability

The PLGA-only scaffold was fabricated by a single-head deposition system. Other PLGA/alginate hybrid printing groups were successfully fabricated by the dual-head deposition system. As presented in Fig. 2, the plotted PLGA line and the pore size of the scaffolds in all groups were 300 and 600 μm, respectively. Live/dead staining of all plotted scaffolds was carried out to determine the rate of cell viability after one week of *in vitro* culturing (Fig. 3). All of the adhered cells survived on the plotted fibers of the PLGA-only scaffold at Day 7. Encapsulated cells in plotted alginate fibers also showed visibility of around 90%. The blending of the cECM and the HA in the alginate did not decrease cell viability after one week. In the SEM images, evenly distributed cells in the spaces between PLGA fibers were observed in plotted cell-laden alginate fibers, while the seeded cells showed a partially spread morphology on the surfaces of the plotted fibers in the PLGA-only control group.

In vitro differentiation potential of HFCPCs

Adipogenic differentiation was evaluated by Oil-red-O staining. Lipid vesicles were observed in the induction group (Fig. 4B). HFCPCs were clearly differentiated into an adipogenic lineage. Osteogenic differentiation was detected by Alizarin red staining. HFCPCs positive for Alizarin red staining was widely distributed throughout the six-well plates (Fig. 4D). *In vitro* chondrogenesis as a pellet culture system was performed to evaluate the chondrogenesis potential of the cells. During chondrogenesis, the pellet size increased due to the production of an extracellular matrix. The pellets of the induction groups were larger and heavier than those of the control group, indicating their superiority in chondrogenesis. Histologically, each cell pellet exhibited a cartilage matrix that was stained with Safranin-O staining (Fig. 4E and F).

cECM blending effects on chondrogenic differentiation in the cartilage layer scaffold

cECM was blended with alginate with cells printed for the cartilage layer of the osteochondral graft. RT-PCR and the GAG

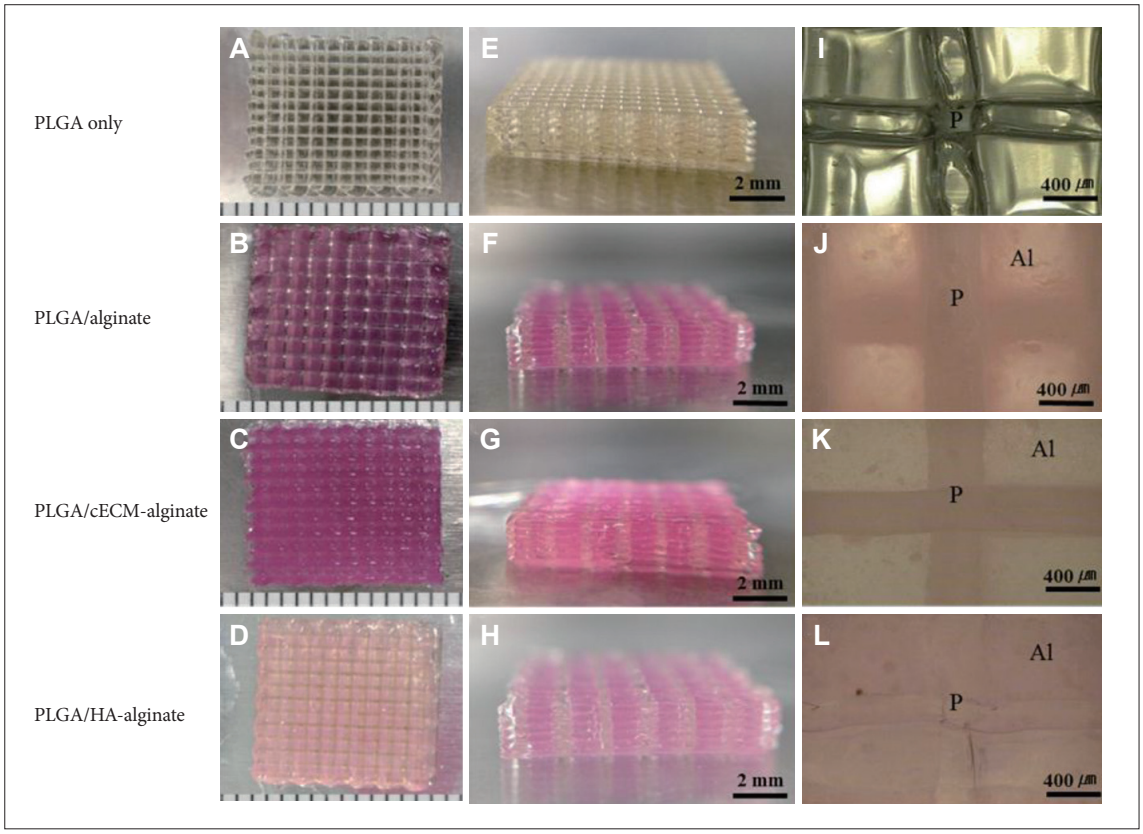

Figure 2. The structure of the SFF-based PLGA only, PLGA and the cell-laden alginate, PLGA and PCP-blended cell-laden alginate, and PLGA and HA-blended cell-laden alginate scaffolds. (A-D) Surface morphologies, and (E-H) side of the scaffold. (I-L) High-magnification image of PLGA and cell-laden alginate fibers. The plotted PLGA line and the pore size of the scaffolds in all groups were 300 and 600 μm, respectively. P: PLGA fiber, Al: alginate fiber, SFF: solid freeform fabrication, PLGA: poly (L-lactic acid-co-glycolic acid), cECM: cartilage-derived ECM, HA: hydroxyapatite.

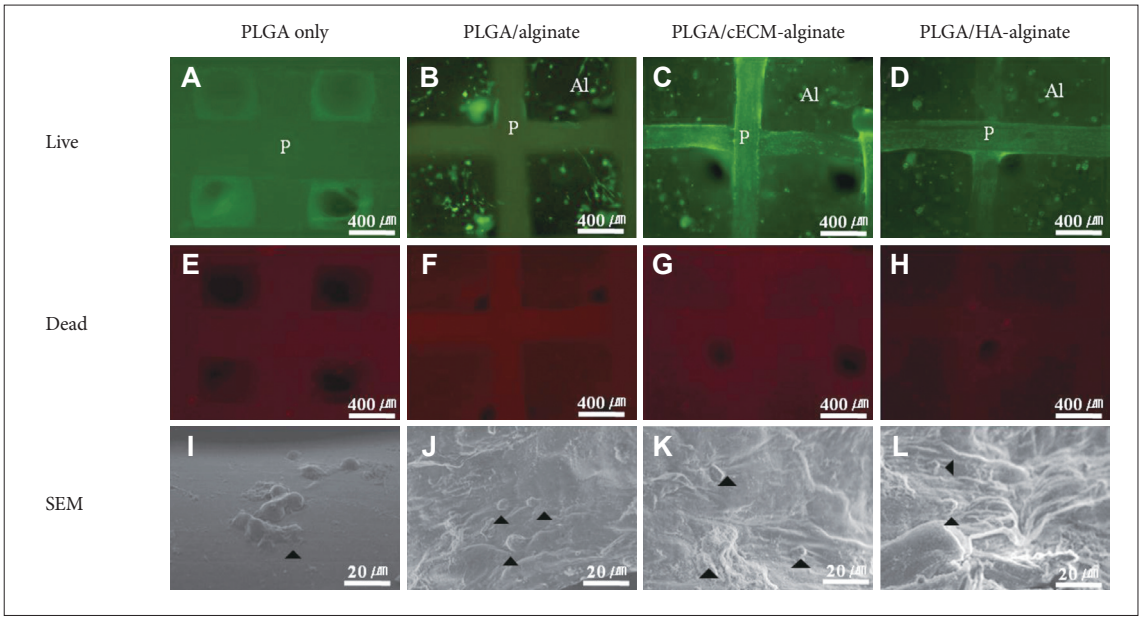

Figure 3. (A-L) Cell viability analysis and SEM morphology. (A and E) Viability at 7 days after cell observations on the PLGA-only scaffold (B, C, and D; F, G, and H) Viability at 7 days after cell-laden alginate printing. Green: live cells, red: dead cells. SEM observation (I) of the attached cell morphology on the plotted PLGA fiber, (J, K, and L) cell-laden morphology in the plotted alginate. ▲: cells, P: PLGA fiber, Al: alginate fiber, SEM: scanning electron microscope, PLGA: poly (L-lactic acid-co-glycolic acid), cECM: cartilage-derived ECM, HA: hydroxyapatite.

content were analyzed at Day 14 after *in vitro* chondrogenic induction. The PLGA/cECM-alginate group showed notably increased gene expression of Col2A1 and aggrean compared to the PLGA-only and the PLGA/alginate samples (Fig. 5A). Moreover, the GAG content in the PLGA/cECM-alginate was 4.5 μg/mg, which was a significantly higher value among the groups (Fig. 5B).

HA blending effects on osteogenic differentiation in a subchondral bone layer scaffold

The ALP activity was used as an important biochemical marker for determining the osteoblast phenotype and the bone differentiation and mineralization characteristics. Thus, the osteogenic differentiation of HFCPCs in three types of scaffolds was also analyzed in terms of the expression levels of the osteogenic markers of ALP and OPN at the level of messenger ribonucleic acid. As shown in Fig. 5C and D, the expression levels of the ALP and OPN genes in the PLGA/HA-alginate were the highest among the three groups. The super-iority of osteogenic differentiation in PLGA/HA-alginate was also proved by a chemical analysis of the ALP activity after two weeks of *in vitro* culturing.

Fabrication of hybrid scaffold

As depicted in Fig. 6, the bi-phasic scaffold consisting of PLGA for the frame and alginate for the HFCPC delivery was successfully fabricated using the SFF technique. In particular, cECM and HA substitutes were blended for cartilage and subchondrodral bone layers, respectively. The structure size of the plotted biphasic scaffold was 3×3×5 mm^3. The biphasic graft showed good integration between the cartilage and subchondral bone layers without structural separation. Furthermore, no structural collapse of the scaffolds was observed during the tissue culturing process.

DISCUSSION

Ideal scaffolds require a stable mimetic hierarchical structure as well as biological features to support the formation of new tissue [18]. Significant advances have been made in the progress of scaffolds fabrication techniques. Nevertheless, fabricated scaffolds using conventional techniques cannot precisely control the pore size, interconnectivity or pore geometry for the specified requirements of tissue regeneration [3,24]. Recently, SFF techniques to create desired structures with good functionality have become a hot issue in tissue engineering as part of the effort to fabricate 3D spatially organized constructs as an advanced form of this technology [9,13]. Plotted 3D scaffolds of synthetic materials have demonstrated good mechanical strength strong enough to maintain structures [9]. PLGA was chosen as the frame structure in this study because SFF-based PLGA scaffolds have shown the successful chondrogenesis of chondrocyte [16]. In addition, the long-lasting degradation be-

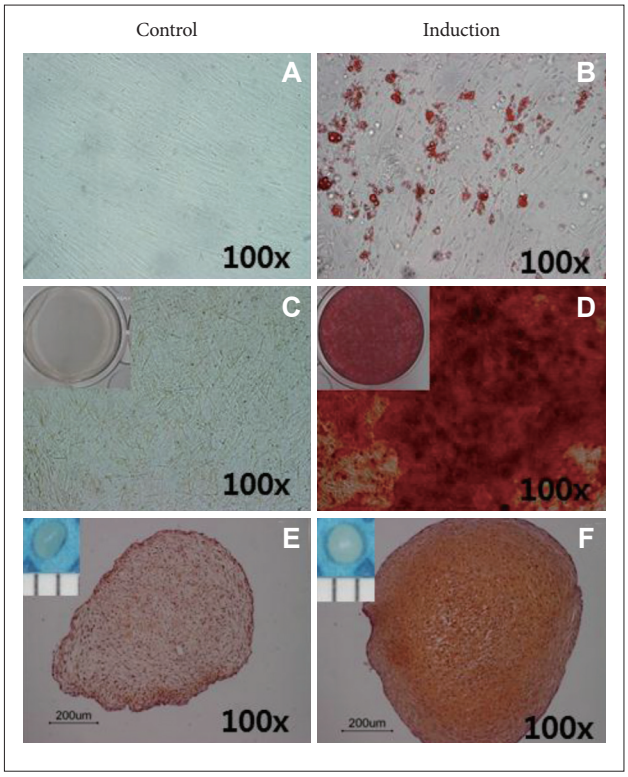

Figure 4. Differentiation of HFCPC. (A and B) Adipogenic differentiated HFCPC with Oil-red O staining. (C and D) Osteogenesis. (E and F) Histology of pellets as determined with Safranin-O staining. HFCPC: human fetal cartilage-derived stem cells.

havior of a 3D-plotted PLGA scaffold was also identified for seven weeks in saline in another study [17]. However, the poor biological features of the PLGA synthetic scaffold were improved by the addition of natural materials to the point that they were even better than those of PCL [25].

Natural hydrogel is commonly utilized for cell deposition in the SFF fabrication system owing to its inherent advantages, such as its bioactivity and biocompatibility [22,23,26]. In particular, the alginate utilized in our study is preferred for SFF fabrication due to its very rapid solidification [27]. Cohen et al. [20] successfully printed cell-laden implants with the alginate hydrogel with SFF technology. Khalil and Sun [22] also reported the ideal conditions of sodium alginate and calcium chloride for SFF bioprinting. However, a 3D-plotted scaffold with alginate only was not suitable for long-term cell culturing owing to its rapid degradation and low mechanical strength. To overcome the limited strength of alginate, the printed PCL structure was combined with a hybrid scaffold for bioprinting [14]. We also found that the alginate-only plotted structure could not withstand a time of two weeks in our pilot study. A long-lasting cell delivery material is needed for long-term culturing to induce mature tissue formation. Thus, we developed both a PLGA and an alginate hybrid plotting system to enable the manufacturing of a biphasic scaffold for application to osteochondral defects. The hybrid printing of alginate and PLGA resulted in stable structural maintenance of more than two weeks (Fig. 2). As another trial for more stable cell printing using alginate, we are now the developing a catechol-added alginate, which is showing very-long-lasting degradation properties in a preliminary study.

During the conditions of tissue formation, maintaining of an appropriate physicochemical environment is essential to promote the tissue regeneration. In particular, tissue-specific ECM can provide the cells with a favorable cellular microenvironment with the appropriate 3D architecture for normal growth and development [28]. The cECM material used here for the cartilage layer contained collagen, glycosaminoglycan and, other adhesion molecules. Cartilage tissue-engineering applications of cECM were developed in our previous studies [29,30]. For instance, the differentiation of planted cells and a high quality of engineered cartilage were generated from ECM materials [31]. ECM materials helped to maintain a chondrogenic phenotype and delay the calcification and hypertrophic changes of engineered cartilage [32]. Moreover, ECM materials can enhance chondrogenic formation in cartilage defects in animals [29,30,33]. Another blended substance, HA, for a subchondral bone layer was also determined to be a suitable material for proliferation and osteoblastic differentiation of mesenchymal stem cells *in vitro* [34]. A HA-combined scaffold-free tissue-engineered construct exhibited earlier restoration of subchondral bone as well as good tissue integration of repaired cartilage in a rabbit osteochondral defect model [35]. Furthermore, pure-alginate-encapsulated stem cells did not show strong evidence of chondrogenic or osteogenic differentiation during *in vitro* culturing [21,36], although the alginate demonstrated high cell viability of more than 83% from plotted cells with alginate when using a multi-nozzle deposition SFF system [22]. In this sense, in order to promote the maturity of osteochondral grafts in our study, cECM or HA substances blended alginates were specifically plotted together with stem cells in cartilage or subchondral bone layers. In the present result, the non-toxicity of cECM and HA substances on cells were proved in a live/dead assay of plotted cell-laden alginate, as presented in Fig. 3. This indicates that cell death did not occur due to the materials or the plotting process used in our system. Regarding the structural stability of the fabricated osteochondral graft, both the cartilage and the subchondral layers were stably plotted up to a height of 5 mm (Fig. 6). Notably, a plotted biphasic structure using the same materials showed strong integration between both cartilage and subchondral bone layers.

Eventually, we also employed HFCPCs as a new cell source for both the chondrogenesis and osteogenesis of osteochondral grafts in the current study. Fetal stem cells are more plastic

than adult stem cells and hence have greater therapeutic potential [37]. The feasibility of using fetal stem cells was confirmed during chondrogenic differentiation and skeletal development assessments for cartilage repair [38]. The stem cells used in this research are fetal tissue-derived stem cells.

As shown in Fig. 4, they can easily be divided into adipocytes, osteocytes, and chondrocytes under conditions with sound differences in a medium. However, without the conditions of the sound difference, they are not divided into bone and cartilage. This tendency is correlated the results of tissue

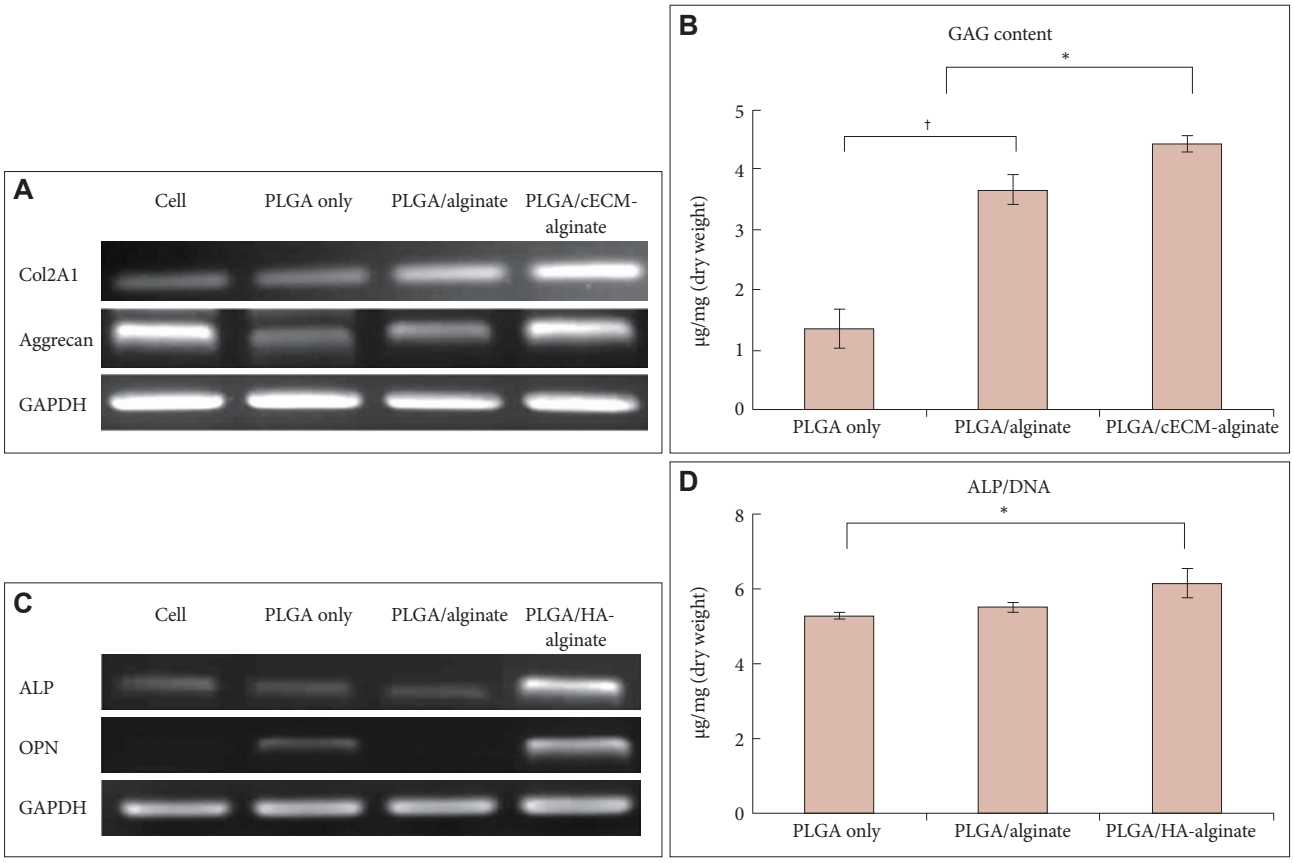

Figure 5. *In vitro* chondrogenesis and osteogenesis assay after 2 weeks of *in vitro* culturing. (A) The RT-PCR gene expressions of chondrogenic-specific markers (B) GAG contents (C). The RT-PCR gene expression of osteogenic-specific markers, (D) ALP activity after osteogenic induction. PLGA/cECM-alginate showed the highest chondrogenetic gene expression levels and GAG content amounts among the groups. PLGA/HA-alginate also showed significantly higher osteogenic differentiation compared to the other samples. Statistically significant differences (*p<0.01 and †p<0.001). PLGA: poly (L-lactic acid-co-glycolic acid), cECM: cartilage-derived ECM, RT-PCR: reverse transcriptase-polymerase chain reaction, GAPDH: glyceraldehyde-6-phosphate dehydrogenase, ALP: alkaline phosphatase, OPN: osteopontin, HA: hydroxyapatite.

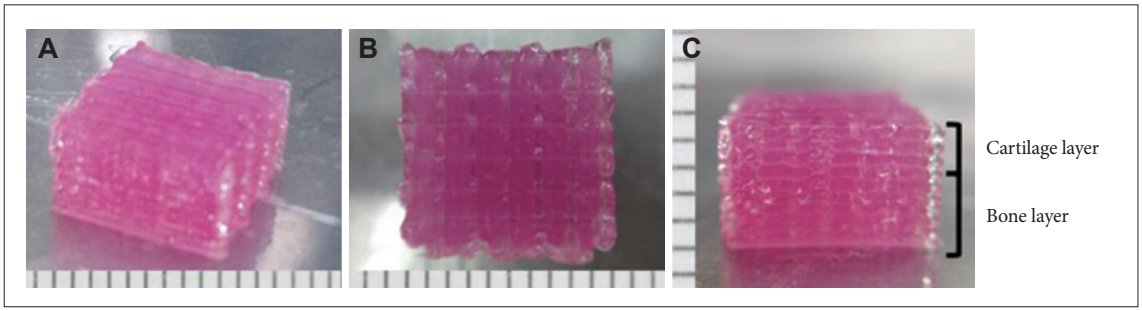

Figure 6. (A) Stably three-dimensional plotted bi-phase scaffold of an osteochondral graft. (B) Front view of the scaffold. (C) Side view of the scaffold. PLGA/cECM-alginate and PLGA/HA-alginate are plotted for the cartilage and the subchondral bone layers, respectively. No structure separation was observed between the two layers during the tissue culturing process. PLGA: poly (L-lactic acid-co-glycolic acid), cECM: cartilage-derived ECM, HA: hydroxyapatite.

diffentiation of biphasic scaffold. HFCPCs in PLGA/cECM-alginate of cartilage layer showed highly expressed chondrogenic gene markers such as type II collagen and aggrecan. In other hand, HFCPCs in PLGA/HA-alginate of bone layer showed the much higher expression of osteogenic gene marker such as ALP and OPN than cartilage layer. the acquired RT-PCR results from this study demonstrated the differential effects of plotting HFCPCs in substances (cECM or HA) blended with alginate for cartilage or subchondral bone layers. However, we unfortunately could not provide the histological staining data because the alginate layers shrunk during the block preparation process in the analysis.

In conclusion, this study identified the plotting feasibility and tissue formation of 3D plotted osteochondral biphasic grafts using PLGA and certain substances (cECM or HA) blended with alginate for the regeneration of osteochondral defects. The utilized bio-printing system includes a dual-printing system that utilizes SFF techniques and a computer-aided modeling system capable of creating heterogeneous osteochondral grafts. Both cartilage and subchondral layers were stably plotted up to a height of 5 mm. The plotted osteochondral graft showed good integration between the cartilage and subchondral bone layers without structural separation. Furthermore, no structural collapse of the 3D plotted scaffolds was observed during the tissue culturing process. A fabricated osteochondral graft with cECM and HA substances showed dominant cartilage and bone tissue formation properties in a differentiation assay. Future studies should focus on modifying the alginate physical properties for long-lasting structural stability. In the meantime, the 3D plotted osteochondral graft will be evaluated in terms of its efficacy from *in vivo* implantation into osteochondral defects.

Acknowledgements

This research was supported by the NRF-2013R1A1A1011040 project and by the Bio & Medical Technology Development Program of the National Research Foundation (NRF) funded by the Ministry of Science, ICT & Future Planning (NRF-2011-0019730).

Conflicts of Interest

The authors have no financial conflicts of interest.

Ethical Statement

The experiments followed the guidelines from the Ajou University Medical Center Institutional Review Board (CRO-07-139, Suwon, Korea).

REFERENCES

1. Obradovic B, Martin I, Padera RF, Treppo S, Freed LE, Vunjak-Novakovic G. Integration of engineered cartilage. J Orthop Res 2001;19:1089-1097.
2. Choi JW, Choi BH, Park SH, Pai KS, Li TZ, Min BH, et al. Mechanical stimulation by ultrasound enhances chondrogenic differentiation of mesenchymal stem cells in a fibrin-hyaluronic acid hydrogel. Artif Organs 2013;37:648-655.
3. Yang S, Leong KF, Du Z, Chua CK. The design of scaffolds for use in tissue engineering. Part I. Traditional factors. Tissue Eng 2001;7:679-689.
4. Holy CE, Shoichet MS, Davies JE. Engineering three-dimensional bone tissue in vitro using biodegradable scaffolds: investigating initial cell-seeding density and culture period. J Biomed Mater Res 2000;51:376-382.
5. Mano JF, Reis RL. Osteochondral defects: present situation and tissue engineering approaches. J Tissue Eng Regen Med 2007;1:261-273.
6. Muschler GF, Nakamoto C, Griffith LG. Engineering principles of clinical cell-based tissue engineering. J Bone Joint Surg Am 2004;86-A:1541-1558.
7. Sharma S, Srivastava D, Grover S, Sharma V. Biomaterials in tooth tissue engineering: a review. J Clin Diagn Res 2014;8:309-315.
8. Harrison RH, St-Pierre JP, Stevens MM. Tissue engineering and regenerative medicine: a year in review. Tissue Eng Part B Rev 2014;20:1-16.
9. Hoque ME, Chuan YL, Pashby I. Extrusion based rapid prototyping technique: an advanced platform for tissue engineering scaffold fabrication. Biopolymers 2012;97:83-93.
10. Chang CC, Boland ED, Williams SK, Hoying JB. Direct-write bioprinting three-dimensional biohybrid systems for future regenerative therapies. J Biomed Mater Res B Appl Biomater 2011;98:160-170.
11. Lee JS, Hong JM, Jung JW, Shim JH, Oh JH, Cho DW. 3D printing of composite tissue with complex shape applied to ear regeneration. Biofabrication 2014;6:024103.
12. Lantada AD, Morgado PL. Rapid prototyping for biomedical engineering: current capabilities and challenges. Annu Rev Biomed Eng 2012;14:73-96.
13. Derby B. Printing and prototyping of tissues and scaffolds. Science 2012;338:921-926.
14. Kundu J, Shim JH, Jang J, Kim SW, Cho DW. An additive manufacturing-based PCL-alginate-chondrocyte bioprinted scaffold for cartilage tissue engineering. J Tissue Eng Regen Med 2013 Jan 24 [Epub]. http://dx.doi.org/10.1002/term.1682.
15. Shim JH, Moon TS, Yun MJ, Jeon YC, Jeong CM, Cho DW, et al. Stimulation of healing within a rabbit calvarial defect by a PCL/PLGA scaffold blended with TCP using solid freeform fabrication technology. J Mater Sci Mater Med 2012;23:2993-3002.
16. Kang SW, Lee SJ, Kim JS, Choi EH, Cha BH, Shim JH, et al. Effect of a scaffold fabricated thermally from acetylated PLGA on the formation of engineered cartilage. Macromol Biosci 2011;11:267-274.
17. Shim JH, Kim JY, Park JK, Hahn SK, Rhie JW, Kang SW, et al. Effect of thermal degradation of SFF-based PLGA scaffolds fabricated using a multi-head deposition system followed by change of cell growth rate. J Biomater Sci Polym Ed 2010;21:1069-1080.
18. Owen SC, Shoichet MS. Design of three-dimensional biomimetic scaffolds. J Biomed Mater Res A 2010;94:1321-1331.
19. Vats A, Tolley NS, Polak JM, Gough JE. Scaffolds and biomaterials for tissue engineering: a review of clinical applications. Clin Otolaryngol Allied Sci 2003;28:165-172.
20. Cohen DL, Malone E, Lipson H, Bonassar LJ. Direct freeform fabrication of seeded hydrogels in arbitrary geometries. Tissue Eng 2006;12:1325-1335.
21. Wang Y, de Isla N, Huselstein C, Wang B, Netter P, Stoltz JF, et al. Effect of alginate culture and mechanical stimulation on cartilaginous matrix synthesis of rat dedifferentiated chondrocytes. Biomed Mater Eng 2008;18(1 Suppl):S47-S54.
22. Khalil S, Sun W. Bioprinting endothelial cells with alginate for 3D tissue constructs. J Biomech Eng 2009;131:111002.
23. Billiet T, Vandenhaute M, Schelfhout J, Van Vlierberghe S, Dubruel P. A review of trends and limitations in hydrogel-rapid prototyping for tissue

engineering. Biomaterials 2012;33:6020-6041.
24. Wake MC, Patrick CW Jr, Mikos AG. Pore morphology effects on the fibrovascular tissue growth in porous polymer substrates. Cell Transplant 1994;3:339-343.
25. Shim JH, Kim AJ, Park JY, Yi N, Kang I, Park J, et al. Effect of solid freeform fabrication-based polycaprolactone/poly(lactic-co-glycolic acid)/collagen scaffolds on cellular activities of human adipose-derived stem cells and rat primary hepatocytes. J Mater Sci Mater Med 2013;24:1053-1065.
26. Wahl DA, Sachlos E, Liu C, Czernuszka JT. Controlling the processing of collagen-hydroxyapatite scaffolds for bone tissue engineering. J Mater Sci Mater Med 2007;18:201-209.
27. Fedorovich NE, Schuurman W, Wijnberg HM, Prins HJ, van Weeren PR, Malda J, et al. Biofabrication of osteochondral tissue equivalents by printing topologically defined, cell-laden hydrogel scaffolds. Tissue Eng Part C Methods 2012;18:33-44.
28. Goessler UR, Hörmann K, Riedel F. Tissue engineering with chondrocytes and function of the extracellular matrix (Review). Int J Mol Med 2004;13:505-513.
29. Jin CZ, Park SR, Choi BH, Park K, Min BH. In vivo cartilage tissue engineering using a cell-derived extracellular matrix scaffold. Artif Organs 2007;31:183-192.
30. Choi KH, Song BR, Choi BH, Lee M, Park SR, Min BH. Cartilage tissue engineering using chondrocyte-derived extracellular matrix scaffold suppressed vessel invasion during chondrogenesis of mesenchymal stem cells in vivo. Tissue Eng Regen Med 2012;9:43-50.
31. Jin CZ, Choi BH, Park SR, Min BH. Cartilage engineering using cell-derived extracellular matrix scaffold in vitro. J Biomed Mater Res A 2010;92:1567-1577.
32. Choi KH, Choi BH, Park SR, Kim BJ, Min BH. The chondrogenic differentiation of mesenchymal stem cells on an extracellular matrix scaffold derived from porcine chondrocytes. Biomaterials 2010;31:5355-5365.
33. Li TZ, Jin CZ, Choi BH, Kim MS, Kim YJ, Park SR, et al. Using cartilage extracellular matrix (CECM) membrane to enhance the reparability of the bone marrow stimulation technique for articular cartilage defect in canine model. Adv Funct Mater 2012;22:4292-4300.
34. Karadzic I, Vucic V, Jokanovic V, Debeljak-Martacic J, Markovic D, Petrovic S, et al. Effects of novel hydroxyapatite-based 3D biomaterials on proliferation and osteoblastic differentiation of mesenchymal stem cells. J Biomed Mater Res A 2015;103:350-357.
35. Shimomura K, Moriguchi Y, Ando W, Nansai R, Fujie H, Hart DA, et al. Osteochondral repair using a scaffold-free tissue-engineered construct derived from synovial mesenchymal stem cells and a hydroxyapatite-based artificial bone. Tissue Eng Part A 2014;20:2291-2304.
36. Hashimoto Y, Adachi S, Matsuno T, Omata K, Yoshitaka Y, Ozeki Y, et al. Effect of an injectable 3D scaffold for osteoblast differentiation depends on bead size. Biomed Mater Eng 2009;19:391-400.
37. van Gool SA, Emons JA, Leijten JC, Decker E, Sticht C, van Houwelingen JC, et al. Fetal mesenchymal stromal cells differentiating towards chondrocytes acquire a gene expression profile resembling human growth plate cartilage. PLoS One 2012;7:e44561.
38. Brady K, Dickinson SC, Guillot PV, Polak J, Blom AW, Kafienah W, et al. Human fetal and adult bone marrow-derived mesenchymal stem cells use different signaling pathways for the initiation of chondrogenesis. Stem Cells Dev 2014;23:541-554.